Integration of multi-level postural balancing on humanoid robots

Sang-Ho Hyon, Rieko Osu and Yohei. Otaka

***Abstract*— This paper discusses an integration issue of multi-level postural balancing on humanoid robot. We give a unified viewpoint of postural balancing, which covers Ankle Strategy to Hip Strategy. Two kinds of distributor of desired ground reaction force to whole-body joint torque are presented. The one distributor leads to a dynamic balancer which covers Hip strategy, with the under-actuated situation. A simple angular momentum regulator is also proposed to stabilize the internal motions due to the joint redundancy. The other distributor leads to a static balancer which lies between Ankle and Hip strategy. Furthermore, this paper demonstrates that replacement of the center of mass feedback with the local joint stiffness makes the robot much stabler for some fast motions. Motivated by the practicability of the static balancer and the strong push-recovery performance of the dynamic balancer, this paper presents a simple integration by superposition of the both balancers on a compliant human-sized biped robot. The simulation and experimental videos are supplemented.**

I. Introduction

A. Motivation

When a human is suddenly pushed forward, he/she can take various actions to recover the balance. Physiologists have been discussing about the three major recovery strategies; (a) Ankle Strategy, (b) Hip Strategy and (c) Step [1][2] . Since human postural control is fundamental full-body motor control for humans, some high level nervous system is supposed to be involved as well as vestibular, somatic and proprioceptive feedback [3][4][5][6]. Actually, the Ankle Strategy is not just joint-stiffness control because there should be anti-gravitational forces, which can be computed by using internal model of body such as mass distribution of the each limb.

The challenge of this paper is to suggest computational models of human postural control by exploiting possible controller realizations on compliant humanoid robots, which interacts with the environment in real-time as humans do [7]. Such attempt is also beneficial to development of human-friendly assistive/rehabilitation devices. Our approach is first implementing the above three strategies on humanoid robot models, and then comparing the results with the human data at different levels of sensory-motor control.

S. Hyon is with JST, ICORP, Computational Brain Project, Honcho 4-1-8, Kawaguchi, Saitama 332-0012, Japan, and ATR Computational Neuroscience Laboratories, Hikaridai 2-2-2, Keihannna Science City, Kyoto, Japan sangho@atr.jp

R. Osu is with ATR Computational Neuroscience Laboratories, Hikaridai 2-2-2, Keihannna Science City, Kyoto, Japan, and National Institute of Information and Communications Technology, Hikaridai 2-2-2, Keihannna Science City, Kyoto, Japan osu@atr.jp

Y. Otaka is with Tokyo Bay Rehabilitation Hospital, Yatsu 4-1-1, Narashino, Chiba 275-0026, Japan otaka119@mac.com

This paper has supplementary material provided by the authors. This is a single MPEG4 format movie which shows the empirical results. The movie is 5 MB in size.

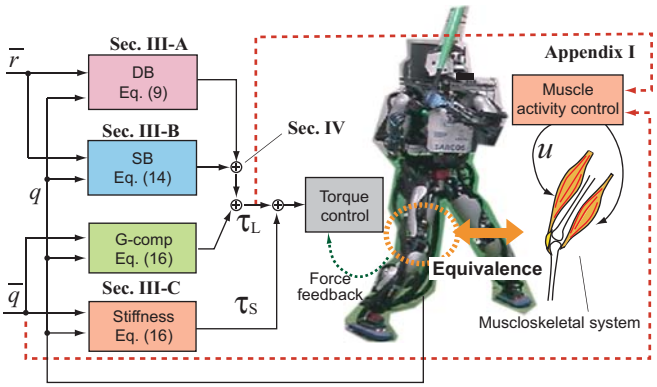

Fig. 1. Overall control architecture of postural balancing. This is composed of dynamic balancer, static balancer, gravity compensation and joint stiffness. The four blocks in the left show each control module, whose details are shown in the indicated sections and equations (ignore some overlapped terms in the equations). $\overline{r}$ is the desired task-space position, and $\overline{q}$ is the desired joint-space position. The outputs of the modules are simply summed up, according to the task objectives.

In robotics, these controllers have been discussed, but in most cases they are independently studied without integration issue (see biped walking literatures). One of the open question is how humans combine (or just switch) these three modules according to the sensory feedback and internal model. A model predictive controller is proposed in [8], and some model-based criteria are proposed in [9][10], based on human model and human gait data.

In [11], we discussed the integration issue in passivity context, and also implemented a simple push-recovery controller from balancing to stepping on a human-sized compliant humanoid robot. This paper continues to discuss the integration issue (comparison with human data is left for the future work). The overview of this paper is shown in Fig. 1.

This paper has three contributions. The first one is a unified viewpoint of postural balancing, which covers Ankle Strategy to Hip Strategy as follows.

- From the causality of the controlled system, the motion of the center of mass (CoM) is determined by the ground reaction force (GRF), and the control problem is how to distribute desired GRF into full-body joint torque. Directly solving the full dynamics leads to a rich balancing controller, which we call Dynamic Balancer (DB) in this paper (1st block in Fig. 1). This balancer is free from so-called "ZMP (Zero Moment Point) criteria" [12], and can be applied to under-actuated

situation, the situation which "Hip" Strategy implies. However, it suffers from the computational cost, internal motions, and singularity. The internal motions appear regardless of the CoM regulation. We show that the internal motions are coming from angular momentum (AM), and the regulation of AM can be achieved by simply adding integral action to the CoM feedback law in the desired GRF.

- Within the limitation of the ZMP criteria, we can use a passivity-based postural control strategy without taking the dynamic effect into account [17]. At the cost of reducing the GRF (hence, the balancing ability), the internal motions due to the redundancy can be suppressed by simple joint damping, which also suppress the angular momentum around CoM. These make the ZMP almost equivalent to center of pressure (CoP). We call this balancing controller as Static Balancer (SB) in this paper (2nd block in Fig. 1). This controller lies between Ankle Strategy and Hip strategy.

The second contribution is a discussion on a stiffness controller superposed by gravity compensator (G-comp) (3rd and 4th block in Fig. 1). This is a simple substitute for the CoM feedback control, resulting in Ankle Strategy. We discuss the advantage and disadvantage of this controller over the CoM feedback from a computational and biological point of view.

The third contribution is a demonstration of a simple integration of SB and DB. Specifically we discuss a superposition of the control outputs (joint torques) of the two control modules (the summation symbol in Fig. 1). We will show the robust push-recovery performance on our humanoid robot.

II. Dynamics

We start with simple planar floating-based models to test ideas, then extend to full-body humanoid model. The experimental hardware are shown in Fig. 2(a) and Fig. 2(b). The former is a planar 4-link acrobat robot, which can control the joint torque by standard analog current feedback [14], where we have succeeded in direct CoM control via inverse dynamics. The latter is a human-sized humanoid robot, CB-i [7], which also provides force control by high-speed force feedback loop. Let us first consider a planar 4-link model comprising torso, thigh, shank and foot as shown in Fig. 3(a). In the later simulation we also use a 3-link model without foot, shown in Fig. 3(b).

We treat balancing control at toe-support or heel-support uniformly, but the equation of motion of the former includes the latter. Therefore, we show only the former one here. Let the toe locate at the origin, and $r_C = [x_C, z_C]^T \in \mathcal{R}^2$ be the position of the CoM, $q := [q_1, q_2, q_3, q_4]^T \in \mathcal{R}^4$ be the posture angles, which combines to $q_C = [r_C, q]^T \in R^6$ where q_1 is the cyclic variable (ignorable coordinate) [13].

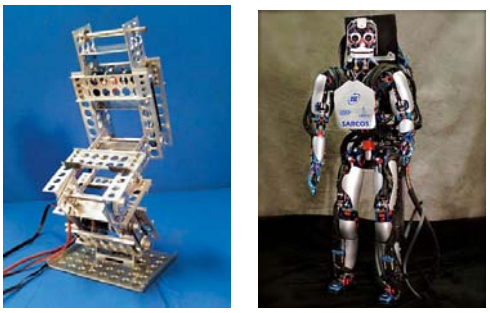

(a) Planar 4-link robot (b) Humanoid robot

Fig. 2. Hardwares for experiments

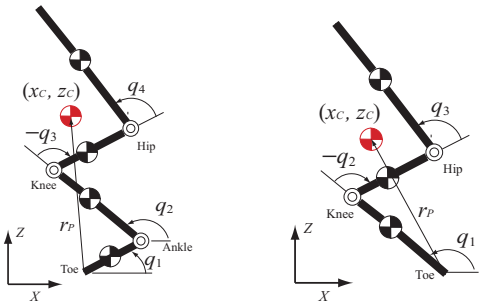

(a) 4-link model (b) 3-link model

Fig. 3. Planar under-actuated models

The constrained equation of motion can be written as

$$\underbrace{\left[\begin{array}{c|c} M & O \\ \hline O & I(q) \end{array}\right]}_{\hat{I}} \underbrace{\left[\begin{array}{c} \ddot{r_C} \\ \hline \ddot{q} \end{array}\right]}_{\ddot{\hat{q}}_C} + \underbrace{\left[\begin{array}{c} O \\ \hline C(q,\dot{q})\dot{q} \end{array}\right]}_{\hat{C}} + \underbrace{\left[\begin{array}{c} MG \\ \hline O \end{array}\right]}_{\hat{G}} = \underbrace{\left[\begin{array}{c} O \\ \hline \tau \end{array}\right]}_{u} + \underbrace{\left[\begin{array}{c} id_2 \\ \hline J_P(q)^T \end{array}\right]}_{\hat{E}^T} f_P \tag{1}$$

and

$$\dot{r}_C + J_P(q)\dot{q} = \underbrace{\left[\begin{array}{c|c} id_2 & J_P(q) \end{array}\right]}_{\hat{E}(q)} \dot{\hat{q}}_C = 0, \tag{2}$$

where id_N is identity matrix of dimension N, O is a zero vector or matrix with the context-wise dimension, $M = \mathrm{diag}(m, m) \in \mathcal{R}^{2\times 2}$ is the mass matrix with m being the total mass, $I(q) \in \mathcal{R}^{4\times 4}$ is the inertia matrix, $C(q,\dot{q})\dot{q} \in \mathcal{R}^4$ is the centrifugal/Colioris term, $G = [0, g]^T \in \mathcal{R}^2$ is the gravity acceleration, $J_P \in \mathcal{R}^{2\times 4}$ is the Jacobian from the toe to the CoM, and $\tau = [\tau_1, \tau_2, \tau_3, \tau_4]^T \in \mathcal{R}^4$ is the applied torque associated to q. The constraint force $f_P \in \mathcal{R}^2$ is the GRF.

Usually, τ_1 is limited or not available. When the foot completely sticks to the ground, this torque plays a role of constraint torque that maintains $q_1 = \dot{q}_1 = 0$. In this case,

this torque together with the GRF f_P determines the position of the CoP. Without any constrain, the above equation shows a simple ballistic flight. See [14] for the details of derivation.

III. A unified interpretation from Ankle Strategy and Hip Strategy

If we define the postural balancing as "the regulation of the ground projection of CoM to the center of supporting region (SR)", it would be useful to control CoM by a new control input $f_u = [f_{ux},\ f_{uz}]^T \in \mathcal{R}^2$, through the linear dynamics

$$M\ddot{r}_C = f_P - MG = f_u. \tag{3}$$

The simplest stabilizing input will be a PD feedback law

$$f_{ux} = -K_P x_C - K_D \dot{x}_C, \tag{4}$$
$$f_{uz} = -K_P(z_C - \overline{z}_C) - K_D \dot{z}_C, \tag{5}$$

with the target height $\overline{z}_C$, which is usually set to equilibrium where the control input can be minimized. Note that one should restrict either f_{ux} and/or f_{uz} to obey the friction constraint $f_{ux} \leq \mu(mg + f_{uz})$ with the friction coefficient μ (in the later simulation we set $\mu = 0.5$).

From Eq. (1) and Eq. (2), f_P can be written by[1]

$$f_P = (\hat{E}\hat{I}^{-1}\hat{E}^T)^{-1} \left\{ \gamma + \hat{E}\hat{I}^{-1}(u - \hat{C} - \hat{G}) \right\} \tag{6}$$

with $\gamma(q, \dot{q}) = \frac{\partial}{\partial q}(\hat{E}\dot{q})\dot{q}$. Hence, we can compute the desired joint torque by substituting Eq. (3) into this equation.

Note, however, this requires inverse operation, which does not give us the unique solution. Nevertheless, the above computation is a fundamental of the *exact* CoM control via GRF. Actually, in the following, we discuss Ankle Strategy and Hip Strategy in a unified mechanism, but with a bit difference of how GRF is distributed into the joint torques.

A. Dynamic solution leads to Hip Strategy

Suppose the robot is in toe-contact. Eq. (6) can be re-written as

$$\underbrace{\hat{E}\hat{I}^{-1}}_{A}(u - \hat{C} - \hat{G}) = \underbrace{-\gamma + (\hat{E}\hat{I}^{-1}\hat{E}^T)(MG + f_u)}_{B}, \tag{7}$$

or

$$\left[\begin{array}{c|c} A_{11} & A_{12} \\ \hline A_{21} & A_{22} \end{array}\right] \left[\begin{array}{c} MG \\ \hline \tau - C\dot{q} \end{array}\right] = \left[\begin{array}{c} B_1 \\ \hline B_2 \end{array}\right]. \tag{8}$$

To give τ_1 freely (including zero), we separate it out, then we obtain

$$\begin{bmatrix} A_{12}(2:4) \\ A_{22}(2:4) \end{bmatrix} \begin{bmatrix} \tau_2 \\ \tau_3 \\ \tau_4 \end{bmatrix} = \begin{bmatrix} B_1 - A_{11}MG - A_{12}C\dot{q} - A_{12}(1)\tau_1 \\ \hline B_2 - A_{21}MG - A_{22}C\dot{q} - A_{22}(1)\tau_1 \end{bmatrix}. \tag{9}$$

The size of the left coefficient matrix is 2×3, and we can solve the equation for (τ_2, τ_3, τ_4) by using pseudo-inverse, which we call dynamic balancer (DB). Moreover, if we use a weighting matrix

$$W = (\mathrm{diag}([m_2,\ m_3,\ m_4]))^{-1}, \tag{10}$$

it prevents the light links from moving fast to rush into the singular posture. Although it is not easy to solve the singularity, the above control torque *exactly* achieves $f_P = MG + f_u$ for given τ_1 and the state $(q, \dot{q})$ *within* the regular region.

Fig. 5 (and **Video 1**) shows the balancing control simulation of the 3-link model (Fig. 3(b)) with $\tau_1 = 0$ and Eq. (4)(5). The link parameters are set similar to the humanoid robot in Fig. 2(b). Since the robot is under-actuated, and the initial CoM is far from the equilibrium, the robot has to move its joints very fast, while avoiding the singularity. We noticed that singularity occurs when the knee joint meets $q_2 \geq 0$. We use a simple joint limit (spring-damper) to avoid the singularity in this simulation. This corresponds to Hip Strategy.

As one can see from the figure and video, the hip joint rotates unboundedly, while the CoM stays at the target position. This shows well-known *internal motion* [15]. The both angular momentums (AM) around the contact point or CoM are converging to constants (see Graph (d)). We cannot avoid the internal motion by tuning parameters. Therefore, the AM together with CoM should be regulated in DB. In [14] we specified the desired AM, then solved its time-derivative together with Eq. (6). Instead of doing this, we will show much simpler solution in Section III-D.

B. Static solution leads to the middle of Hip and Ankle Strategy

If the toe and heel do not leave the ground, we can use τ_1 as the control input. In this case, quasi-static solution is available, which we call static balancer (SB). If we put $\gamma \approx 0$ and $\hat{C} \approx 0$ into Eq. (6), we can obtain the control torque

$$\tau = J_P^T(f_v + MG), \tag{11}$$
$$f_v = f_u + (J_P I^{-1} J_P^T)^{-1} M^{-1} f_u, \tag{12}$$

which leads to

$$f_P \approx f_u + MG \tag{13}$$

Moreover, if we put the additional damping term to the right-hand-side of Eq. (11) and further simplifies it, we have

$$\tau = J_P^T(f_u + MG) - D\dot{q}. \tag{14}$$

With this controller we can prove the actual GRF asymptotically approaches to the desired one:

$$f_P \to f_u + MG \quad (t \to \infty) \tag{15}$$

This is a passivity-based contact force control for redundant legged robots proposed in [16]. For balancing case, the desired GRF can be designed as Eq. (4). When $f_u = 0$ (no CoM feedback), the controller becomes a (full-body) G-comp.

[1] By substituting Eq. (6) into Eq. (1), we can obtain the reduced dynamics of dimension 4.

The resultant controller is a full-body torque controller, not corresponding to Ankle Strategy, nor Hip Strategy. See [17] for the actual performance of the controller (14) (with additional optimization), which was applied to a full-body humanoid robot. To make SB work properly, the ZMP must lie within SR. Therefore we restrict f_u so that the desired CoP does not cross the bound of SR [11]. This is not the case for DB.

C. Replacing the CoM feedback to local stiffness leads to Ankle Stragety

The Ankle Strategy was originally meant for stabilizing control of a single inverted pendulum that represents a global human posture. It has a unique upright equilibrium posture $q = q_e$ where $x_C = 0$. The stabilization is achieved by a local PD control torque around the pivot, the ankle joint. In addition, an integral action or feedforward input should be used if the target posture is not q_e.

For multi-DoF humanoid model, the equilibrium posture is not unique. If the equilibrium posture q_e is given in advance, we can implement local joint stiffness control around that posture. As a result, we can replace the original controller Eq. (14) + Eq. (4) with a simpler one:

$$\tau = J_P(q)^T MG - D\dot{q} - K(q - q_e), \tag{16}$$

where K is a stiffness matrix to be designed or learned [18].

Below we discuss how this controller is useful from a computational point of view. First of all, note that the computational cost is the same because we use full-body G-comp that requires forward kinematics. The problem lies in its practicability. The CoM feedback (Eq. (14) with Eq. (4)) is flexible, but it makes the robot fluctuate even in the equilibrium posture because of the noise in the CoM estimation (including the orientation measurement). Contrary, the response of Eq. (16) is much faster than the CoM feedback because the stiffness torque is implemented in the local joint controller. The schematic illustration comparing with the CoM feedback is shown in Fig. 4.

The first G-comp term in Eq. (16) has also the same delay, therefore, the update of the motor command is relatively slow. However, as described in Appendix I, the delayed motor command generates stiffness around the target posture. We think this noise-robust controller is suitable for some fast coordinated motions, although some physiology papers [19][20] argues that these are coupled.

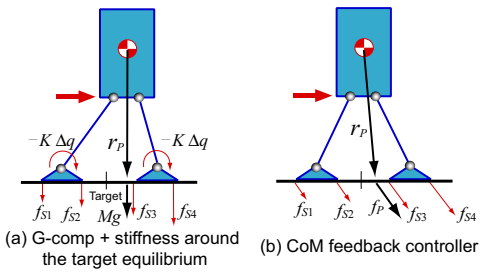

Fig. 4. Two balancing schemes against unknown external side-force. (a) Simple balancing control scheme with G-comp and stiffness. (b) CoM feedback control with G-comp. For the details of the optimal contact force distribution f_{Sj} $(j = 1, 2, ...)$, see [17].

Video 2 and **Video 3** show the experimental results of fast upper-body motions with torso twisting during quite stance [21], under the two different balancing schemes discussed above. The latter is much stabler than the former one. This is because the lower limbs do not need to move much in this particular motion example. Otherwise, the desired equilibrium posture q_e should be replaced with the equilibrium trajectory $q_e(t)$ [25].

D. Stabilization of angular momentum by integral action

As we have seen in Section III-A, merely stabilizing CoM does not solve the internal motions. On the other hand, a passivity-based solution in Section III-B can suppress the internal motions, but the region of attraction is limited by CoP up to SR.

Here we take a look at AM. The third line of the equation of motion Eq. (1),

$$I_1\ddot{q} + C_1\dot{q} = \tau_1 + J_{P1}^T f_P, \tag{17}$$

where I_1 and C_1 are the third row vector of the inertia matrix I and colinear matrix C, respectively (neither includes the cyclic variable q_1), and $J_{P1} = [-z_C,\ x_C]^T$ is the sub-matrix of $J_P = [J_{P1} \mid J_{P2}]$.

Since the AM around CoM is represented by $P_C = I_1\dot{q}$, Eq. (17) can be re-written as

$$\dot{P}_C = \tau_1 + J_{P1}^T f_P. \tag{18}$$

On the other hand, the AM around the contact point is expressed, by definition, as

$$P_0 = P_C + r_C \times m\dot{r}_C, \tag{19}$$

and its time-derivative is given by

$$\begin{aligned} \dot{P}_0 &= \dot{P}_C + m(z_C\ddot{x}_C - x_C\ddot{z}_C) \\ &= \dot{P}_C + z_C f_x - x_C(f_z - mg). \end{aligned} \tag{20}$$

Substituting Eq. (18) into Eq. (20) yields

$$\begin{aligned} \dot{P}_0 &= (-z_C f_x + x_C f_z + \tau_1) + z_C f_x - x_C(f_z - mg) \\ &= \tau_1 + x_C mg. \end{aligned} \tag{21}$$

From Eq. (19) we reach the following statement. Since $r_C \times m\dot{r}_C \to 0$ when the CoM is asymptotically stable, it can happen that $P_0 \neq 0$ if $P_C \neq 0$. This is the internal motions we have seen in Section III-A.

Consequently, from Eq. (21) it is found that we should use

$$f_{ux} = -K_P x_C - K_D\dot{x}_C - K_I \int (\tau_1 + x_C mg)dt, \tag{22}$$

instead of Eq. (4), to regulate AM. Thus we can achieve $P_0 \to 0$, which means the allowed motion is asymptotically restricted to the manifold $I_1\dot{q} = 0$.

Fig. 6 (and **Video 4**) shows the result of the proposed controller (22). The conditions are exactly the same as the previous simulation (Fig. 5) except for the additional integral action. The internal motions completely disappeared.

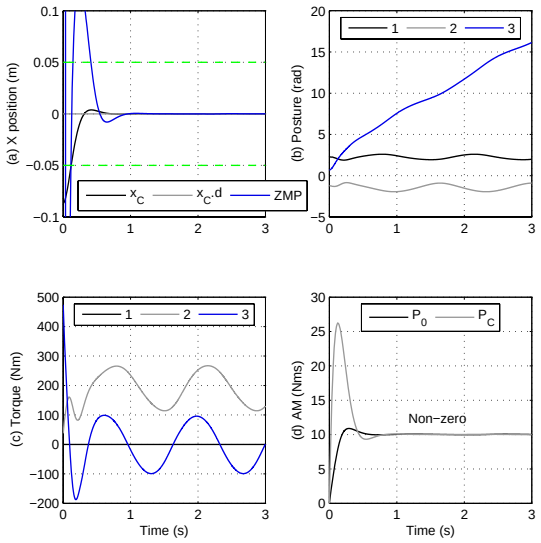

Fig. 5. Three-link model under-actuated balancing simulation (**Video 1**)

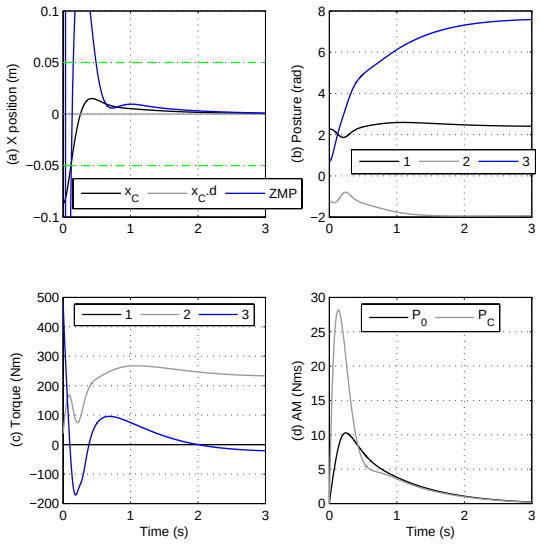

Fig. 6. With angular momentum regulation by integral action (**Video 4**)

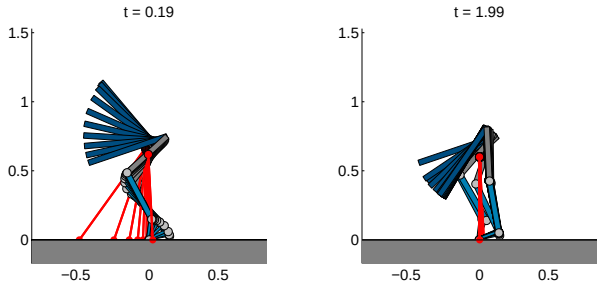

(a) Initial motion (b) Final

Fig. 7. Animation corresponding Fig. 8

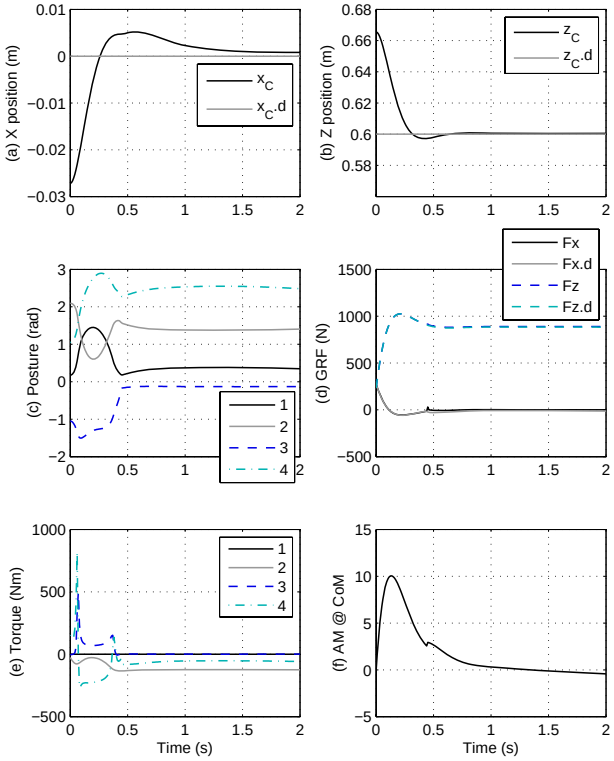

Fig. 8. 4-link model under-actuated balancing simulation

The similar balancing simulations are conducted using the 4-link model with the toe contact. The result is shown in Fig. 7 and Fig. 8 (and **Video 5**), where the weight matrix Eq. (10) is adopted. Interestingly, the recovery motion looks like human's behavior. The CoM and ZMP rapidly approach to the origin (toe) within 0.2 s as shown in Fig. 7(a), and then slowly converge[2] as shown in Fig. 7(b). Note that no torque is applied around the toe (see $\tau_1 = 0$ in Graph (e)). The AM rapidly increases from the initial value (zero) as the CoM is pulled back to origin, and then converges to zero as the internal motion (joint motion) converges. The global error response is determined by a linear feedback controller (22). If we want, we can shape the response curve by modifying the desired GRF. Note there is a discontinuous change around 0.45 s. This is because of the knee joint hitting its limit. Since we use a simple spring-damping model for the limit, there are small errors in the GRF (Graph (d)). The torso is strongly tilted from the initial upright posture. It is not difficult to expect the amount of the tilt can be reduced if we put the arms to the body because the arm will rotate to the same direction.

The actual region of attraction is limited by physical constraints such as maximum torque, range of joint angle, etc. Although some analysis on a simple pendulum model with a flywheel is useful [22], it would be difficult to

[2]It would be natural to set the target of CoM to a position a bit behind the toe. Then, the robot can relax at the static equilibrium. We didn't do this here simply because it was tedious to simulate the heel contact, but see Section IV.

take everything into account for full-body humanoid robot without off-line optimization or try-and-error based learning. Nevertheless, it is worth to implement the DB together with SB on our humanoid robot to see the performance and the limitation, which is shown in the next section.

IV. Integration on Humanoid Robot

This section presents a simple integration of SB and DB and applies to a human-sized humanoid robot. Since we have no solid evidences on how humans use these two modules, we first implement and test the both on the actual robot, and then get back to the theory.

The motivation to use SB is its simplicity, practicability and safety. But it is not strong. Actually, it loses the controllability of CoM once its projection locates outside SR. On the other hand, DB suffers from difficulties in implementation: difficult to derive the dynamic model, and difficult to compute (measure) the necessary dynamics to compensate Therefore, we use the SB as a *default*, and combine the DB in a safe way. Specifically, we tested a simple superposition of SB and DB, where the DB is computed for a reduced 2-link *acrobot* [23] model, where the control input is available only for the hip joint (ankle joint is free). Different from the controller for 3-link or 4-link model in Section III-A, the acrobot controller is free from the control singularity; the equation is simple; no need to use the weighting matrix. The 2-link model is the reduced model of the humanoid robot, where the first link is composed of the shank and thigh, and the second link is the torso.

The control output from DB is just superposed to the hip joint. Similar integration can be found in [24], but a difference is that we limit the desired CoP for SB, but not do that for DB to take advantage of its strong recovery performance. Also, we are applying *full-body* SR (not local stiffness control) with the optimized contact force control for all the time.

Below we show some simulation and experimental results on a full-body humanoid robot. **Video 6** shows the simulation result, where forward and backward pushes ($\pm$300 N to the pelvis during 0.1 s) are applied. The arm joints are just commanded zero torque with a small damping, and the head is orientation controlled. Fig. 9 show the corresponding simulation data. See the caption for the details of the data. Without DB, the robot could not recover the balance. Without SB, the robot could not keep its posture, and the upper body rapidly rotated, which made the normal GRF small enough for the robot to lose its contact with the ground.

Fig. 10 show an experimental result with the same controller. Strong forward/backward pushes have been applied from human operator to the robot pelvis. Graph (f) shows the torque output from the 2-link DB module, which is distributed to the both right and left hip joints. A large input is required for a "strong" backward push applied at t = 33 s (indicated by bPush2). The required torque for the hip joint exceeds 200 Nm. On the other hand, in the case of the similar "strong" forward push at 42.5 s (indicated by fPush3), the hip torque is about -150 Nm. The compensation appears to

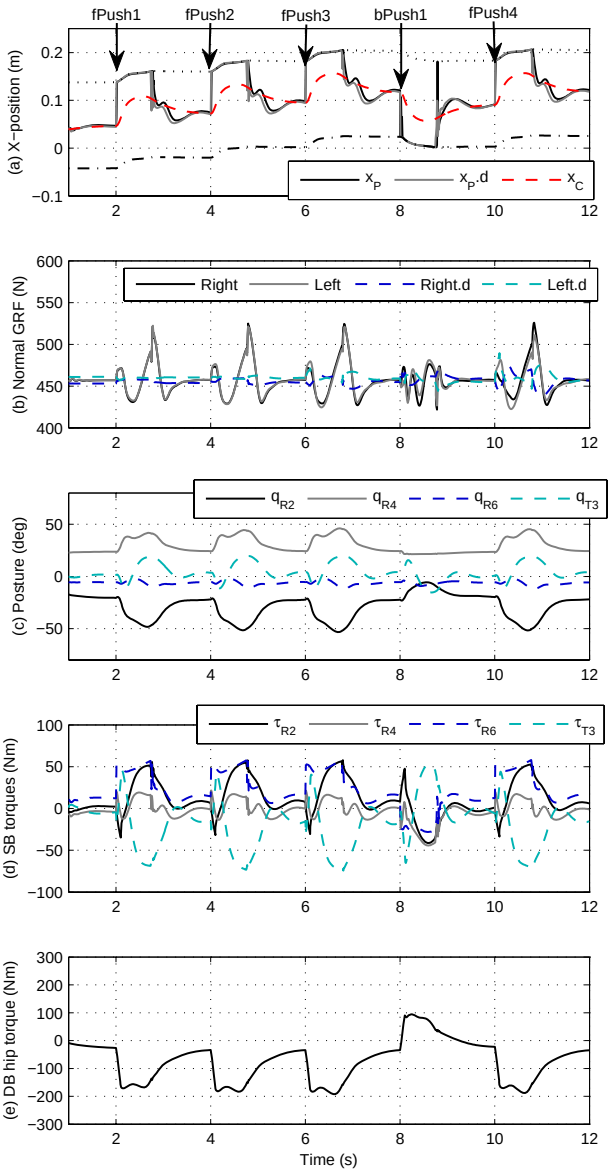

Fig. 9. Simulation data of push-recovery control by SB and DB. Multiple pushes have been applied to the robot torso. (a) xC is CoM, xP and xP.d are the actual and desired CoP, which do not exceed SR (upper and lower bounds, which are slightly shifting upward because of the slippage). The forward pushes (fPush1, fPush2, fPush3, fPush4) and the single backward push (bPush1) are indicated. Compare with **Video 6**. (b) Actual GRF does not match to the desired because of the superposition. (c) Desired and actual CoM height. (d) joint angles for the right leg (q_{R2}:hip, q_{R4}:hip, q_{R6}:ankle) and the torso pitch (q_{T3}). (e) Control output from SB module. The subscripts have the same meaning as Graph (d). (f) Control output from DB module. Comparing with τ_{R2}, the sign of the DB torque is opposite to the SB torque for the initial stage of the push-recovery.

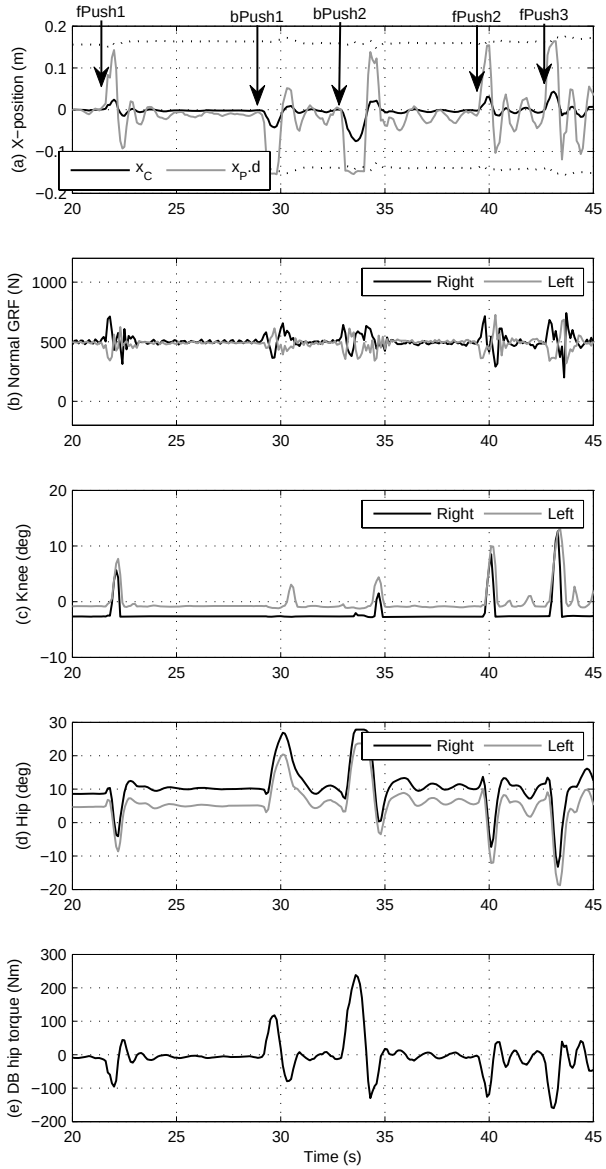

Fig. 10. Experimenta data of push-recovery control by SB and DB. The symbols are the same as Fig. 9. Large peaks mean that three-times forward pushes and twice backward pushes (fPush1, bPush1, bPush2, fPush2, fPush3) have been applied to the robot pelvis from the human operator. When bPush2 is applied, the actual hip torque saturated (not shown in graphs).

the knee joint (Graph (c)). Fig. 11 shows the snap shots of the recovery motion when pushed the torso (see **Video 7**).

V. Conclusion and Future Work

The motivating idea of using passivity-based controller (SB) for postural balancing was its simplicity and practicability. On the other hand, the purpose of deriving complex controller (DB) was to test its actual performance. From the practical and safety reason, in this paper we integrated the both by simple superposition. Surprisingly, the performance has been greatly improved compared with the case only SB is

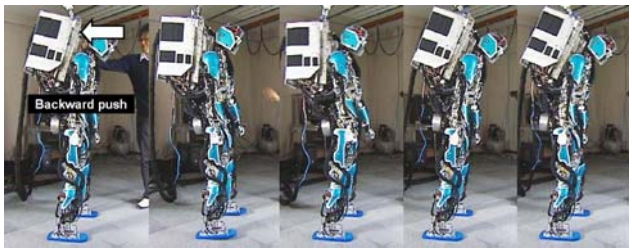

Fig. 11. Typical behavior of superposition of SB and DB (**Video 7**)

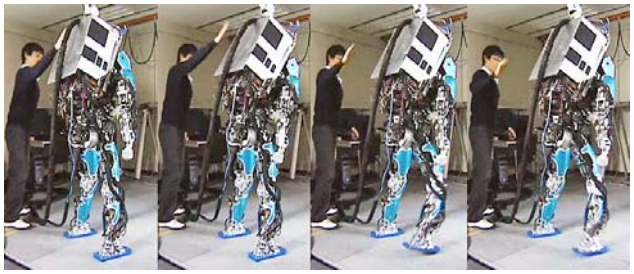

Fig. 12. Combined push-recovery with stepping (**Video 7**)

used. However, dynamic motions are expected to be learned by robot itself [25]. Our future effort will be devoted to this work. On the other hand, once the balancing performance is improved, it becomes easy to combine the step strategy for re-balancing. Fig. 12 (**Video 7**) shows one of the re-balancing experiment. The same *symmetric* foot placement strategy in [16] has been applied. We expect the robust push-recovery controller leads to robust walking, which we believe a starting point for optimal walking via learning.

VI. Acknowledgments

The authors would like to thank the National Institute of Communication Telecommunication (NICT), Japan. The authors gratefully acknowledge N. Nakano (NICT) for the experimental setups, and Prof. C. G. Atkeson (CMU), Dr. D. Bentivegna (CMU) and Prof. H. Herr (MIT) for helpful discussions.

References

[1] F. B. Horak and L. M. Nashner, "Central programming of postural movements: adaptation to altered support-surface configurations," *Journal of Neurophysiology*, vol. 55, no. 6, pp. 1369–1381, 1986.

[2] A. Winter, David, *A.B.C. (Anatomy, Biomechanics and Control) of Balance During Standing and Walking*. Waterloo Biomechanics, 1995.

[3] L. R. Squire, D. Berg, F. Bloom, S. D. Lac, A. Ghosh, and N. C. Spitzer, Eds., *Fundamental Neuroscience*. Academic Pr, 2008.

[4] R. J. Peterka, "Sensorimotor integration in human postural control," *J Neurophysiol*, vol. 88, no. 3, pp. 1097–118, 2002.

[5] H. van der Kooij, R. Jacobs, B. Koopman, and H. Grootenboer, "A multisensory integration model of human stance control," *Biol Cybern*, vol. 80, no. 5, pp. 299–308, 1999.

[6] P. G. Morasso and V. Sanguineti, "Ankle muscle stiffness alone cannot stabilize balance during quiet standing," *J Neurophysiol*, vol. 88, no. 4, pp. 2157–62, 2002.

[7] M. Kawato, "From 'Understanding the Brain by Creating the Brain' towards manipulative neuroscience," *Philosophical Transactions of the Royal Society*, vol. 363, no. 1500, pp. 2201–2214, 2008.

[8] P. G. Morasso, L. Baratto, R. Capra, and G. Spada, "Internal models in the control of posture," *Neural Netw*, vol. 12, no. 7-8, pp. 1173–1180, 1999.

[9] A. D. Kuo, "An optimal control model for analyzing human postural balance," *Biomedical Engineering, IEEE Transactions on*, vol. 42, no. 1, pp. 87 – 101, 1995.
[10] M. B. Popovic, A. Goswami, and H. Herr, "Ground reference points in legged locomotion: Definitions, biological trajectories and control implications," *The International Journal of Robotics Research*, vol. 24, no. 12, pp. 1013 – 1032, 2005.
[11] S. Hyon and G. Cheng, "Disturbance rejection for biped humanoids," in *IEEE International Conference on Robotics and Automation*, Roma, Italy, 2007, pp. 2668–2675.
[12] M. Vukobratović and B. Borovac, "Zero-moment point - thirty five years of its life," *International Journal of Humanoid Robotics*, vol. 1, no. 1, pp. 157–173, 2004.
[13] D. T. Greenwood, *Classical Dynamics*. Dover, 1977.
[14] S. Hyon, N. Yokoyama, and T. Emura, "Back handspring of a multi-link gymnastic robot - reference model approach," *Advanced Robotics*, vol. 20, no. 1, pp. 93–113, 2006.
[15] R. M. Murray, Z. Li, and S. S. Sastry, *A Mathematical Introduction to Robotic Manipulation*. CRC Press, 1994.
[16] S. Hyon and G. Cheng, "Passivity-based full-body force control for humanoids and application to dynamic balancing and locomotion," in *IEEE/RSJ International Conference on Intelligent Robots and Systems*, Beijing, China, Oct. 2006, pp. 4915–4922.
[17] S. Hyon, J. G. Hale, and G. Cheng, "Full-body compliant human-humanoid interaction: Balancing in the presence of unknown external forces," *IEEE Transactions on Robotics*, vol. 23, no. 5, pp. 884–898, 2007.
[18] E. Burdet, R. Osu, D. Franklin, T. Milner, and M. Kawato, "The central nervous system stabilizes unstable dynamics by learning optimal impedance," *Nature*, vol. 414, pp. 446–449, 2001.
[19] K. Masani, M. R. Popovic, K. Nakazawa, M. Kouzaki, and D. Nozaki, "Importance of body sway velocity information in controlling ankle extensor activities during quiet stance," *J Neurophysiol*, vol. 90, no. 6, pp. 3774–82, 2003.
[20] I. D. Loram, S. M. Kelly, and M. Lakie, "Human balancing of an inverted pendulum: is sway size controlled by ankle impedance?" *J Physiol*, vol. 532, no. Pt 3, pp. 879–91, 2001.
[21] S. Hyon, J. Moren, and M. Kawato, "Toward humanoid batting: Prediction and fast coordinated motion," in *RSJ Annual Conference*, 2008, pp. AC2J2–01.
[22] J. Pratt, J. Carff, S. Drakunov, and A. Goswami, "Capture point: A step toward humanoid push recovery," in *IEEE-RAS International Conference on Humanoid Robots*, Genova, Italy, 2006, pp. 200–207.
[23] M. Spong, "The swing up control problem for the acrobot," *IEEE Control Systems Magazine*, vol. 15, no. 1, pp. 49–55, 1995.
[24] B. Stephens, "Integral control of humanoid balance," in *IEEE/RSJ 2007 International Conference on Intelligent Robots and Systems*, 2007.
[25] S. Hyon, J. Morimoto, and G. Cheng, "Hierarchical motor learning and synthesis with passivity-based controller and phase oscillator," in *IEEE International Conference on Robotics and Automation*, Pasadena, USA, pp. 2705–2710.
[26] N. Hogan, "Adaptive control of mechanical impedance by coactivation of antagonist muscles," *Automatic Control, IEEE Transactions on*, vol. 29, no. 8, pp. 681 – 690, Aug 1984.
[27] J. Yamaguchi and A. Takanishi, "Development of a biped walking robot having antagonistic driven joints using nonlinear spring mechanism," in *IEEE International Conference on Robotics and Automation*, vol. 1, 1997, pp. 185–192.

APPENDIX I
BIOLOGICAL EVIDENCE OF SUPERPOSITION

Here we briefly explain the superposition in Eq. (16) from a biological point of view. We adopt a simple musculoskeletal system model proposed by Hogan [26]. Fig. 13 shows a single joint model. With this model, we can compute the desired motor command (neural activity) for isometric muscles $\overline{u}_1$, $\overline{u}_2$ when some desired one-parameter joint trajectory $\overline{q}(t)$ (angle displacement from the rest posture) and desired load torque $\overline{\tau}_L(t)$ are given. For example, the anti-gravitational torque to support own weight will be the most

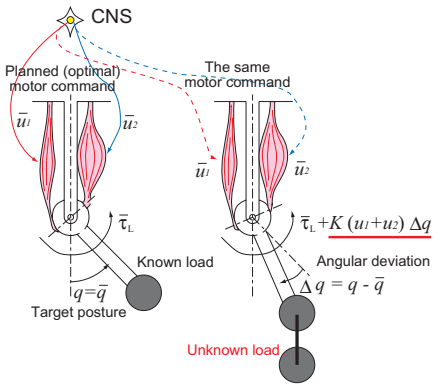

Fig. 13. Operation of the musculoskeletal system model under load. (Left) Planned (optimal) motor command for some given target posture $\overline{q}$ and load. The load torque is indicated by $\overline{\tau}$. (Right) The net torque under unknown load with the same motor command. This observation motivates the implementation of superposition in the whole-body force controller given by Eq. (16).

fundamental load torque for human postural control. Using the musculoskeletal model, the motor command is computed as

$$\overline{\tau}_L(t) = T_0(u_1 - u_2) - K(u_1 + u_2)\overline{q}(t), \tag{23}$$

where K is the angular stiffness, and T_0 is the maximum torque in the rest position (see [26]).

We can solve the for the "optimal" motor command $\overline{u}$ from Eq. (23) (using the Kuhn-Tucker conditions), which is applied to the muscles in a *feedforward* manner. Then, the actual applied torque becomes

$$\tau = T_0(\overline{u}_1 - \overline{u}_2) - K(\overline{u}_1 + \overline{u}_2)q. \tag{24}$$

When $q(t) = \overline{q}(t)$, the joint torque satisfies $\tau = \overline{\tau}_L(t)$. Otherwise, the joint torque becomes

$$\tau = \overline{\tau}_L + K(\overline{u}_1 + \overline{u}_2)\Delta q \tag{25}$$

where $\Delta q = q - \overline{q}$ is the joint angle error.

This results in a superposition of feedforward and proportional feedback control laws for the target joint trajectory. This observation supports the implementation of superposition in a simple balancer given by Eq. (16).

The desired loads and postures are assumed to be given by the task-space control center. If the robot has artificial muscles in its joints [27], then a lower-level control center generates the necessary motor commands for the muscles, as shown in the right block in Fig. 1. In our humanoid robot, torque control is implemented as high-speed force feedback control.